

Acceleration of Plasma Flows Due to Inverse Dynamo Mechanism

Swadesh M. Mahajan¹

Institute for Fusion Studies, The University of Texas at Austin, Austin, Texas 78712

Nana L. Shatashvili²

Plasma Physics Department, Tbilisi State University, Tbilisi 380028, Georgia

Abdus Salam International Center for Theoretical Physics, Trieste, Italy

Solomon V. Mikeladze and Ketevan I. Sigua

Andronikashvili Institute of Physics, Georgian Academy of Sciences, Georgia

ABSTRACT

The "inverse-dynamo" mechanism — the amplification/generation of fast plasma flows by short scale (turbulent) magnetic fields via magneto-fluid coupling is recognized and explored. It is shown that large-scale magnetic fields and flows are generated simultaneously and proportionately from short scale fields and flows. The stronger the short-scale driver, the stronger are the large-scale products. Stellar and astrophysical applications are suggested.

Subject headings: acceleration of particles — magnetic fields — MHD — instabilities — Stars: magnetic fields — Stars: atmospheres — Stars: chromospheres — Stars: coronae — ISM: magnetic fields

The generation of large scale magnetic fields (primarily from short scale velocity fields) defines the standard "dynamo" mechanism. The dynamo action seems to be a very pervasive phenomenon; in fusion devices as well as in astrophysics (stellar atmosphere, MHD jets) one sees the emergence of macro-scale magnetic fields from an initially turbulent system. The relaxation observed in the Reverse Field pinches is a vivid illustration of the dynamo in action. Search for interactions that may result in efficient dynamo action is one of the most flourishing fields in plasma astrophysics. The myriad phenomena taking place in the stellar atmospheres (heating of the corona, the stellar wind etc.) could hardly be understood without knowing the origin and nature of the magnetic field structures weaving the corona.

¹Electronic mail: mahajan@mail.utexas.edu

²Electronic mail: shatash@ictp.trieste.it nanas@iberiapac.ge

The conventional dynamo theories concentrate on the generation of macroscopic magnetic fields in charged fluids. With time the dynamo theories have invoked more and more sophisticated physics models — from the kinematic to the magneto hydrodynamic (MHD) to, more recently, the Hall MHD (HMHD) dynamo. In the latter theories the velocity field is not specified externally (as it is in the kinematic case) but evolves in interaction with the magnetic field. Naturally both MHD and HMHD "dynamo" theories encompass, in reality, the simultaneous evolution of the magnetic and the velocity fields. If the short-scale turbulence can generate long-scale magnetic fields, then under appropriate conditions the turbulence could also generate macroscopic plasma flows. In this context, a quotation from a recent study is rather pertinent: the structures/magnetic elements produced by the turbulent amplification are destroyed/dissipated even before they are formed completely (Bellot Rubio *et al.* 2001; Socas-Navarro & Manso Sainz 2005; Blackman 2005) creating significant flows or leading to the heating.

If the process of conversion of short-scale kinetic energy to long-scale magnetic energy is termed "dynamo" (D) then the mirror image process of the conversion of short-scale magnetic energy to long-scale kinetic energy could be called "inverse dynamo" (ID). It is convenient to somewhat extend the definitions – the D (ID) process connotes the generation of the macroscopic magnetic field (flow) independent of the mix of the short-scale energy (magnetic and kinetic).

Within the framework of a simple HMHD system, we demonstrate in this paper that the Dynamo and the Inverse Dynamo processes operate simultaneously — whenever a large scale magnetic field is generated there is a concomitant generation of a long scale plasma flow. Whether the macroscopic flow is weak (sub-Alfvénic) or strong (super-Alfvénic) with respect to the macroscopic field will depend on the composition of the turbulent energy. We shall derive the relationships between the generated fields and the flows and discuss the conditions under which one or the other process is dominant. In Sec.1 we display an analytical calculation based on the conversion of short scale magnetic and kinetic energy into macroscopic fields and flows. In particular, we dwell on the inverse dynamo mechanism: the permanent dynamical feeding of the flow kinetic energy through an interaction of the turbulent magnetic field structures with weak flows (seed kinetic energy). In Sec.2 we illustrate that the theoretically derived processes do indeed take place by presenting simulation results from a general two fluid code that includes dissipation.

1. Theoretical Model Analysis

The physical model exploited for flow generation/acceleration is simplified HMHD – a minimal model that entertains two interacting scales that can be quite disparate; the macroscopic scale of the system is generally much larger than the ion skin depth, the intrinsic scale of HMHD at which ion kinetic inertia effects become important (Mahajan & Yoshida 1998; Mahajan *et al.* 2001; Ohsaki *et al.* 2002; Yoshida *et al.* 2004). In HMHD the ion and electron flow velocities are different being \mathbf{v} and $\mathbf{v}_e = (\mathbf{v} - \mathbf{j}/en)$ in the limit of zero electron inertia. In its dimensionless form, HMHD comprises of

$$\frac{\partial \mathbf{b}}{\partial t} = \nabla \times \left[[\mathbf{v} - \alpha_0 \nabla \times \mathbf{b}] \times \mathbf{b} \right], \quad (1)$$

$$\frac{\partial \mathbf{v}}{\partial t} = \mathbf{v} \times (\nabla \times \mathbf{v}) + (\nabla \times \mathbf{b}) \times \mathbf{b} - \nabla \left(p + \frac{v^2}{2} \right). \quad (2)$$

with the standard normalizations: the density n to n_0 , the magnetic field to the some measure of the ambient field B_0 and velocities to the Alfvén velocity V_{A0} . We note that the Hall current contributions become significant when the dimensionless Hall coefficient $\alpha_0 \lambda_{i0}/R_0$ (R_0 – the characteristic scale length of a system and $\lambda_{i0} = c/\omega_{i0}$ is the collisionless skin depth) satisfies the condition: $\alpha_0 > \eta$, where η is the inverse Lundquist number for the plasma. For a typical solar plasma, in the corona, the chromosphere and the transition region (TR), this condition is easily satisfied (α_0 is in the range $10^{-10} - 10^{-7}$ for densities within $(10^{14} - 10^8) \text{ cm}^{-3}$ and $\eta = c^2/(4\pi V_{A0} R_\odot \sigma) \sim 10^{-14}$, where R_\odot is solar radius, σ is the plasma conductivity). In such circumstances, the Hall currents modifying the dynamics of the microscopic flows and fields could have a profound impact on the generation of macroscopic magnetic fields (Mininni *et al.* 2003) and fast flows (Mahajan *et al.* 2002; Mahajan *et al.* 2005).

In the following analysis α_0 will be absorbed by choosing the normalizing length scale to be λ_{i0} . Let us now assume that our total fields are composed of some ambient seed fields and fluctuations about them,

$$\mathbf{b} = \mathbf{H} + \mathbf{b}_0 + \tilde{\mathbf{b}}, \quad \mathbf{v} = \mathbf{U} + \mathbf{v}_0 + \tilde{\mathbf{v}} \quad (3)$$

where \mathbf{b}_0 , \mathbf{v}_0 are the equilibrium fields and \mathbf{H} , \mathbf{U} and $\tilde{\mathbf{b}}$, $\tilde{\mathbf{v}}$ are, respectively, the macroscopic and microscopic fluctuations.

Notice that our ambient fields are allowed to have a component at a microscopic scale. We will invoke the Double Beltrami (DB) pair for the analytic part of the paper. The DB configurations are known to be robust and accessible, through a variational principle, for a variety of conditions including inhomogeneous densities (Mahajan & Yoshida 1998). Non constant density cases do display many interesting phenomena (Mahajan *et al.* 2002;

Mahajan *et al.* 2005), but the dynamo and inverse dynamo actions can be very adequately described by the analytically tractable constant density system. We shall, therefore, choose the following DB pair (obeying the concomitant Bernoulli condition $\nabla(p_0 + \mathbf{v}_0^2/2) = \text{const}$)

$$\frac{\mathbf{b}_0}{a} + \nabla \times \mathbf{b}_0 = \mathbf{v}_0, \quad \mathbf{b}_0 + \nabla \times \mathbf{v}_0 = d\mathbf{v}_0, \quad (4)$$

as a representative ambient state. The general solution is expressible in terms of the single Beltrami fields ($\nabla \times \mathbf{G}(\lambda) = \lambda \mathbf{G}(\lambda)$):

$$\mathbf{b}_0 = C_+ \mathbf{G}(\lambda_+) + C_- \mathbf{G}(\lambda_-), \quad (5)$$

$$\mathbf{v}_0 = (a^{-1} + \lambda_+) C_+ \mathbf{G}(\lambda_+) + (a^{-1} + \lambda_-) C_- \mathbf{G}(\lambda_-). \quad (6)$$

Here the parameters a and d are set by the invariants of the system; the magnetic $h_1 = \int (\mathbf{A} \cdot \mathbf{b}) d^3x$ and the generalized $h_2 = \int (\mathbf{A} + \mathbf{V}) \cdot \nabla \times (\mathbf{A} + \mathbf{V}) d^3x$ helicities (Mahajan & Yoshida 1998; Mahajan *et al.* 2001). The inverse scale lengths and λ_+ and λ_- are fully determined in terms of a and d : $\lambda_{\pm} = \frac{1}{2}[(d - a^{-1}) \pm \sqrt{(d + a^{-1})^2 - 4}]$. As the DB parameters a and d vary, λ_{\pm} can range from real to complex values of arbitrary magnitude¹.

Our primary interest is the creation of macro fields from the ambient micro fields. Some what later we will assume, for simplicity, that our zeroth order fields are wholly at the microscopic scale. This allows us to create a hierarchy in the micro fields, the ambient fields are much greater than the fluctuations at the same scale; assuming $|\tilde{\mathbf{b}}| \ll |\mathbf{b}_0|$, $|\tilde{\mathbf{v}}| \ll |\mathbf{v}_0|$ yields the following evolution equations:

$$\begin{aligned} \partial_t \mathbf{U} &= \mathbf{U} \times (\nabla \times \mathbf{U}) + \nabla \times \mathbf{H} \times \mathbf{H} \\ &+ \left\langle \mathbf{v}_0 \times (\nabla \times \tilde{\mathbf{v}}) + \tilde{\mathbf{v}} \times (\nabla \times \mathbf{v}_0) + (\nabla \times \mathbf{b}_0) \times \tilde{\mathbf{b}} + (\nabla \times \tilde{\mathbf{b}}) \times \mathbf{b}_0 \right\rangle \\ &- \langle \nabla(\mathbf{v}_0 \cdot \tilde{\mathbf{v}}) \rangle - \nabla \left(p + \frac{\mathbf{U}^2}{2} \right), \end{aligned} \quad (7)$$

$$\frac{\partial \tilde{\mathbf{v}}}{\partial t} = -(\mathbf{U} \cdot \nabla) \mathbf{v}_0 + (\mathbf{H} \cdot \nabla) \mathbf{b}_0, \quad (8)$$

$$\frac{\partial \tilde{\mathbf{b}}}{\partial t} = (\mathbf{H} \cdot \nabla) \mathbf{v}_{e0} - (\mathbf{U} \cdot \nabla) \mathbf{b}_0, \quad (9)$$

$$\frac{\partial \mathbf{H}}{\partial t} = \nabla \times \left\langle [\tilde{\mathbf{v}}_e \times \mathbf{b}_0] + \mathbf{v}_{e0} \times \tilde{\mathbf{b}} \right\rangle + \nabla \times [(\mathbf{U} - \nabla \times \mathbf{H}) \times \mathbf{H}], \quad (10)$$

where the brackets $\langle \dots \rangle$ denote the spatial averages and $\mathbf{v}_{e0} = \mathbf{v}_0 - \nabla \times \mathbf{b}_0$. This set can be regarded as a closure model of the Hall–MHD equations, which are now general since

¹ In the analysis below we will use λ for the short-scale and μ for the large scale structures.

the feedback of the micro-scale is consistently included in the evolution of both \mathbf{H} and \mathbf{U} ; the role of the Hall current (especially in the dynamics of the micro-scale) is also properly accounted for (Mininni *et al.* 2003).

We now choose the constants a and d so that the two Beltrami scales become vastly separated. This is the astrophysically relevant regime (the size of the structure is much greater than the ion skin depth). We shall deal with two extreme cases for highly disparate scales: : (i) $a \sim d \gg 1$, $(a - d)/ad \ll 1$ ($\lambda \sim d$, $\mu \sim (a - d)/ad$), and (ii) $a \sim d \ll 1$, $(a - d)/ad \gg 1$ ($\lambda \sim (a - a^{-1})$, $\mu \sim (d - a)$).

Consistent with the main objectives of this paper, we will now assume that the original equilibrium is predominantly short-scale (condition applicable for many astrophysical systems), i.e, the basic reservoir from which we will generate large scale fields is, indeed, at a totally different scale. Neglecting the large scale component altogether, the assumed equilibria becomes simpler with the velocity and magnetic fields linearly related as

$$\mathbf{v}_0 = \mathbf{b}_0 (\lambda + a^{-1}) \quad (11)$$

leading to

$$\mathbf{v}_{e0} = \mathbf{v}_0 - \nabla \times \mathbf{b}_0 = \mathbf{b}_0 a^{-1} \quad (12)$$

$$\dot{\tilde{\mathbf{b}}} = (a^{-1} \mathbf{H} - \mathbf{U}) \cdot \nabla \mathbf{b}_0 \quad (13)$$

$$\dot{\tilde{\mathbf{v}}} = (\mathbf{H} - (\lambda + a^{-1}) \mathbf{U}) \cdot \nabla \mathbf{b}_0. \quad (14)$$

Notice the preponderance of nonlinear terms in the evolution equations for \mathbf{U} and \mathbf{H} . These terms will certainly play a very important part in the eventual saturation of the macroscopic fields, but in the early acceleration stage when the ambient short scale energy is much greater than the newly created macroscopic energy, these terms will not be significant. Deferring the fully nonlinear to a later stage, we shall limit ourselves to a "linear" treatment here. Neglecting the nonlinear terms and manipulating the system of equations, we readily derive (after "solving" for and eliminating the short scale fluctuating fields)

$$\ddot{\mathbf{H}} \simeq \left(1 - \frac{\lambda}{a} - \frac{1}{a^2}\right) \langle \nabla \times (\mathbf{H} \cdot \nabla) \mathbf{b}_0 \times \mathbf{b}_0 \rangle, \quad (15)$$

$$\ddot{\mathbf{U}} \simeq \langle (\lambda + a^{-1}) (\lambda \dot{\tilde{\mathbf{v}}} - \nabla \times \dot{\tilde{\mathbf{v}}}) - (\lambda + a^{-1}) \nabla (\mathbf{b}_0 \cdot \dot{\tilde{\mathbf{v}}}) \times \mathbf{b}_0 \rangle - \langle (\lambda \dot{\tilde{\mathbf{b}}} - \nabla \times \dot{\tilde{\mathbf{b}}}) \times \mathbf{b}_0 \rangle. \quad (16)$$

where the spatial averages are yet to be performed. We use the standard isotropic ABC solution of the single Beltrami system,

$$b_{0x} = \frac{b_0}{\sqrt{3}} [\sin \lambda y + \cos \lambda z],$$

$$\begin{aligned} b_{0y} &= \frac{b_0}{\sqrt{3}} [\sin \lambda z + \cos \lambda x], \\ b_{0z} &= \frac{b_0}{\sqrt{3}} [\sin \lambda x + \cos \lambda y]. \end{aligned} \quad (17)$$

to compute the spatial averages. After some tedious but straightforward algebra, we arrive at the final acceleration equations

$$\ddot{\mathbf{U}} = \frac{\lambda}{2} \frac{b_0^2}{3} \nabla \times \left[\left(\left(\lambda + \frac{1}{a} \right)^2 - 1 \right) \mathbf{U} - \lambda \mathbf{H} \right] \quad (18)$$

$$\ddot{\mathbf{H}} = -\lambda \frac{b_0^2}{3} \left(1 - \frac{\lambda}{a} - \frac{1}{a^2} \right) \nabla \times \mathbf{H}. \quad (19)$$

where b_0^2 measures the ambient short scale magnetic energy (also the kinetic energy because of (11)). The coefficients in these equations are determined by a and d ($\lambda = \lambda(a, d)$).

We see that, to leading order, \mathbf{H} evolves independently of \mathbf{U} but the reverse is not true: the evolution of \mathbf{U} does require knowledge of \mathbf{H} .

In the dynamo context, the Hall-currents in the micro-scale are known to modify the α coefficient so that it survives the standard cancellation of the kinetic and magnetic contributions for Alfvénic perturbations (Mininni *et al.* 2002). It is also known that, depending on the state of the system, the Hall effect (by replacing the bulk kinetic helicity by the electron flow helicity) can cause large enhancement or suppression of the dynamo action as compared to the standard MHD.

Writing (18) and (19) as

$$\ddot{\mathbf{H}} = -r (\nabla \times \mathbf{H}), \quad \ddot{\mathbf{U}} = \nabla \times [s \mathbf{U} - q \mathbf{H}], \quad (20)$$

where

$$r = \lambda \frac{b_0^2}{3} (1 - \lambda a^{-1} - a^{-2}), \quad s = \lambda \frac{b_0^2}{6} [(\lambda + a^{-1})^2 - 1], \quad q = \lambda^2 \frac{b_0^2}{6}, \quad (21)$$

and Fourier analyzing, one obtains

$$-\omega^2 \mathbf{H} = -i r (\mathbf{k} \times \mathbf{H}), \quad -\omega^2 \mathbf{U} = i \mathbf{k} \times (s \mathbf{U} - q \mathbf{H}). \quad (22)$$

yielding the growth rate,

$$\omega^4 = r^2 k^2, \quad \omega^2 = -|r|(k), \quad (23)$$

at which \mathbf{H} and \mathbf{U} increase. The growing macro fields are related to one another by

$$\mathbf{U} = \frac{q}{s+r} \mathbf{H}. \quad (24)$$

We shall now show how a choice of a and d fixes the relative amounts of microscopic energy in the ambient fields and consequently in the nascent macroscopic fields \mathbf{U} or \mathbf{H} . We examine our two extreme cases:

(i) For $a \sim d \gg 1$, the inverse short scale $\lambda \sim a \gg 1$ implying $\mathbf{v}_0 \sim a \mathbf{b}_0 \gg \mathbf{b}_0$, i.e, the ambient short-scales fields are primarily kinetic. These type of conditions may be met in stellar photospheres, where the turbulent velocity field at some stage can be dominant although some \mathbf{b}_0 is present as well. For these parameters, it can be easily seen that the generated macro-fields have precisely the opposite ordering, $\mathbf{U} \sim a^{-1} \mathbf{H} \ll \mathbf{H}$. This is an example of the straight dynamo mechanism. Short scale fields with kinetic dominance create, preferentially, large scale fields that are magnetically dominant — super-Alfvénic "turbulent flows" lead to steady flows that are equally sub-Alfvénic (remember we are using Alfvénic units). It is extremely important, however, to emphasize that the dynamo effect (dominant in this regime) must always be accompanied by the generation of large-scale plasma flows. This realization can have serious consequences for defining the initial setup for the later dynamics in the stellar atmosphere. The presence of an initial large-scale velocity field during the flux emergence processes is, for instance, always guaranteed by the mechanism exposed above. The implication is that all models of chromosphere heating / particle acceleration should take into account the existence of large-scale primary plasma flows (even weak) and their self-consistent coupling (see (Mahajan *et al.* 2001; Ohsaki *et al.* 2002; Mahajan *et al.* 2005) and references therein).

(ii) For $a \sim d \ll 1$ the inverse short scale $\lambda \sim a - a^{-1} \gg 1$. Consequently $\mathbf{v}_0 \sim a \mathbf{b}_0 \ll \mathbf{b}_0$, and the ambient energy is mostly magnetic. These conditions might pertain in certain domains in the photospheres or chromospheres, where the turbulent velocity field may exist, but the turbulent magnetic field is the dominant component. This short-scale magnetically dominant initial system creates large-scale fields $\mathbf{U} \sim a^{-1} \mathbf{H} \gg \mathbf{H}$ that are kinetically abundant. The situation has fully reversed from the one discussed in the previous example — starting from a strongly sub-Alfvénic turbulent flow, the system generates a strongly super-Alfvénic large-scale flow; this mode of conversion could be called the "inverse dynamo" mechanism. In the region of a given astrophysical system where the fluctuating/turbulent magnetic field is initially dominant, the magneto-fluid coupling induces efficient/significant acceleration and part of the magnetic energy will be transferred to steady plasma flows. The eventual product of the inverse dynamo mechanism is a steady super-Alfvénic flow — large flow accompanied by a weak magnetic field. It is tempting to stipulate that inverse dynamo

may be the explanation for the observations that fast flows are generally found in weak field regions of the solar atmosphere (Woo & Habbal & Feldman 2004).

This simple analysis has led to, what we believe, are several far-reaching results: (1) the dynamo and "reverse dynamo" mechanisms have the same origin – they are manifestation of the magneto–fluid coupling; (2) The proportionality of \mathbf{U} and \mathbf{H} implies that they must be present simultaneously, and the greater the large–scale magnetic field (generated locally), the greater the large–scale velocity field (generated locally); (3) the growth rate of the large–scale fields scales directly with the ambient turbulent energy $\sim b_0^2 (v_0^2)$. Thus, the larger the initial turbulent magnetic energy, the stronger the acceleration of the flow. We believe that these novel results will surely help in advancing our understanding of the evolution of large–scale magnetic fields and their opening up with respect to the fast particle escape from the stellar coronae. This effect may also have important impact on the dynamical and continuous kinetic energy supply of plasma flows observed in various astrophysical systems.

As the macro–scale fields (both velocity and magnetic) become sufficiently large, the nonlinear terms (ignored in the above analysis) will come into play and significantly change the evolution of the coupled flow–field system; at this stage the dissipation effects may also be important. In the section below we present one illustrative example of a more general dynamical event of flow acceleration in the solar atmosphere in order to demonstrate the complexity of the evolution of the large–scale fields.

2. A Simulation Example

We now present some representative results from our 2.5 D numerical simulation of the general two-fluid equations in Cartesian Geometry (Mahajan *et al.* 2001). For a description of the code, please, see also (Mahajan *et al.* 2005). The idea is to understand aspects of these results in the light of the analytical theory of acceleration developed in the previous section. The simulation system is somewhat different because of the existence of an ambient embedding macroscopic field. We find that the basic qualitatively features of the dynamo and inverse dynamo mechanisms do not change much but the algebra is considerably more complicated and will be presented in a longer paper later.

The simulation system contains several effects not included in the analysis; it has, for instance, dissipation and heat flux in addition to the vorticity and the Hall terms. Transport coefficients for heat conduction and viscosity are taken from (Braginski 1965).

The simulation presented here deals with the trapping and amplification of a primary flow impinging on a single closed–line structure. The choice of initial conditions is guided

by the observational evidence (Aschwanden *et al.* 2001; Woo & Habbal & Feldman 2004) of the self-consistent process of acceleration and trapping/heating of plasma particles in the finely structured solar atmosphere. The simulation begins with a weak symmetric up-flow (initially Gaussian, $|\mathbf{V}|_{0max} \ll C_{s0}$) with its peak located in the central region of a single closed magnetic field structure (location of field maximum $B_{0z} = 100 G$ – upper plot of Fig.1 for the vector potential (flux function) defining the 2D arcade). This field was assumed to be initially uniform in time. The magnetic field is represented as : $\mathbf{B} = \nabla A_y + B_z \hat{\mathbf{z}}$ with $\mathbf{A}(0; A_y; 0)$; $\mathbf{b} = \mathbf{B}/B_{0z}$; $b_x(t, x, z \neq 0) \neq 0$. From numerous runs on the flow-field evolution, we have chosen to display the results corresponding to the following initial and boundary flow parameters: $V_{0max}(x_o, z = 0) = V_{0z} = 2.18 \cdot 10^5 \text{ cm/s}$; $n_{0max} = 10^{12} \text{ cm}^{-3}$; $T(x, z = 0) = const = T_0 = 10 \text{ eV}$. The background plasma density is $n_{bg} = 0.2n_{0max}$. In simulations $n(x, z, t = 0) = n/n_{0max}$ is an exponentially decreasing function of z . Experience was a guide to for imposing the following boundary condition, $\partial_x \mathcal{K}(x = \pm\infty, z, t) = 0$ which was used with sufficiently high accuracy for all parameters $\mathcal{K}(\mathbf{A}, T, \mathbf{V}, \mathbf{B}, n)$. The initial velocity field has a pulse-like distribution (middle and lower plots of Fig.1) with a time duration $t_0 = 100 \text{ s}$.

It is found that:

- (1) acceleration is significant in the vicinity of the magnetic field–maximum (originally present or newly created during the evolution) with strong deformation of field lines and energy re-distribution; initially part of the flow is trapped in the maximum field localization area, accumulated, cooled and accelerated (plots corresponding to $t = 100 \text{ s}$ in Fig.2). The accelerated flow reaches $\gtrsim 100 \text{ km/s}$ value in less than 100 s (in agreement with recent observations (Schrijver *et al.* 1999; Seaton *et al.* 2001; Ryutova & Tarbell 2003) and references therein).
- (2) after this stage the flow passes through a series of quasi-equilibria. In this relatively extended era ($\sim 1000 \text{ s}$) of stochastic/oscillating acceleration, the intermittent flows continuously acquire energy (see Fig.3 for the flow kinetic and magnetic energy maxima).
- (3) The flow starts to accelerate again (Fig.3(a-c) for velocity field evolution). This process is completely consistent with the analytical prediction; the acceleration is highest in the strong field regions (newly generated, Fig.2). At this moment the accelerated daughter flows (large-scale) are decoupled from the mother flow carrying currents and modifying the initial arcade field creating new b_{max} localization areas that span the region between $\lesssim 0.05 R_s$ and $\sim 0.01 R_s$ from the interaction surface. Fluctuations in magnetic energy (Fig.3(e)) as well as in thermal energy (Fig.2) lead to the flow kinetic energy growth.

The extensive simulation runs also show that when dissipation is present, the hall term (proportion to α_0), through the mediation of short-scale physics, plays a crucial role in the acceleration/heating processes. The existence of initial fast acceleration in the region

of maximum localization of the original magnetic field, and the creation of new areas of large-scale magnetic field localization (Fig.2, panel for A_y) with simultaneous transfer of the magnetic energy (oscillatory, short-scale) to flow kinetic energy (Fig.2, panel for $|\mathbf{V}|$ and Fig.3 results) are manifestations of the combined effects of the dynamo and inverse dynamo phenomena. The maintenance of quasi-steady flows for rather significant period is also an effect of the continuous energy supply from fluctuations (due to the Hall and vorticity effects). These flows are likely to provide a very important input element for understanding the finely structured atmospheres with their richness of dynamical structures as well as for the mechanisms of heating, and possible escape of plasmas.

3. Conclusions and Acknowledgments

From an analysis of the two-fluid equations, we have extracted, in this paper, the "inverse-dynamo" mechanism — the amplification/generation of fast plasma flows in astrophysical systems with initial turbulent (short scale) magnetic fields. This process is simultaneous with, and complimentary to the highly explored dynamo mechanism. It is found (both analytically and numerically) that the generation of large-scale flows is an essential consequence of the magneto-fluid coupling, and is independent of the initial and boundary conditions. The generation of large scale magnetic fields and flows goes hand in hand; the greater the large-scale magnetic field (generated locally) the greater the large-scale velocity field (generated locally). The acceleration due to the inverse dynamo is directly proportional to the initial turbulent magnetic energy. When the turbulent magnetic field is initially dominant, a major part of its energy transforms to large-scale flow energy; a weak large-scale magnetic field is generated along with.

The inverse dynamo mechanism, providing an unfailing source for large-scale plasma flows, is likely to be an important mechanism for understanding a host of phenomena in astrophysical systems.

Authors would like to thank Dr. R. Miklaszewski for helpful suggestions for the improved code construction. Authors thank Abdus Salam International Centre for Theoretical Physics, Trieste, Italy. The study of SMM was supported by USDOE Contract No. DE-FG03-96ER-54366. The work of NLS, SVM, KIS was supported by ISTC Project G-633.

REFERENCES

Aschwanden, M.J., Poland A.I., and Rabin D.M. 2001a, *Ann. Rev. Astron. Astrophys.*, 39, 175.

Bellot Rubio, L.R., Rodriguez Hidalgo, I., Collados, M., Khomenko, E. and Ruiz Cobo, B. 2001, *ApJ*, 560, 1010.

Blackman, E.G. 2005, *Phys. of Plasmas*, 12, 012304.

Braginski, S.I. "Transport processes in a plasma," in *Reviews of Plasma Physics*, edited by M. A. Leontovich. Consultants Bureau, New York, (1965), Vol.1, p.205.

Mahajan, S.M., and Yoshida, Z. 1998, *Phys. Rev. Lett.*, 81, 4863.

Mahajan, S.M., Miklaszewski, R., Nikol'skaya, K.I., and Shatashvili, N.L. 2001, *Phys. Plasmas*, 8, 1340.

Mahajan, S.M., Nikol'skaya, K.I., Shatashvili, N.L. & Yoshida, Y. 2002, *ApJ*, 576, L161.

Mahajan, S.M., Shatashvili, N.L., Mikeladze, S.M. and Sigua, K.I. 2005, ArXive: astro-ph/0502345.

Mininni, P. D., Gomez, D. O. and Mahajan, S.M. 2002, *ApJ*, 567, L81.

Mininni, P. D., Gomez, D.O. and Mahajan, S.M. 2003, *ApJ*, 584, 1120.

Ohsaki, S., Shatashvili, N.L., Yoshida, Z., and Mahajan, S.M. 2002, *ApJ*, 570.

Ryutova, M. and Tarbell, T. 2003, *Phys. Rev. Lett.*, 90, 191101. 2002, *ApJ*, 564, 1048.

Schrijver, C.J., Title, A.M., Berger, T.E., Fletcher, L., Hurlburt, N.E., Nightingale, R.W., Shine, R.A., Tarbell, T.D., Wolfson, J., Golub, L., Bookbinder, J.A., Deluca, E.E., McMullen, R.A., Warren, H.P., Kankelborg, C.C., Handy B.N., and DePontieu, B. 1999, *Solar Phys.*, 187, 261.

Seaton, D.B., Winebarger, A.R., DeLuca, E.E., Golub, L., and Reeves, K.K. 2001, *ApJ*, 563, L173.

Socas-Navarro, H. and Sainz, M. 2005, *ApJ*, 620, L71.

Woo, R., Habbal, S.R. and Feldman, U. 2004, *ApJ*, 612, 1171.

Yoshida, Z., Ohsaki, S. and Mahajan, S.M. 2004, *Phys. Plasmas*, 11, 3660.

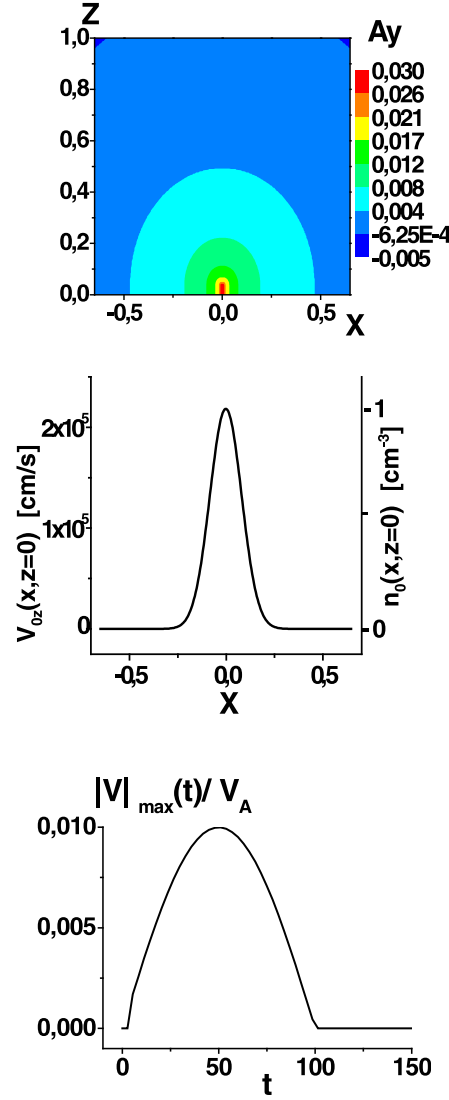


Fig. 1

Fig. 1.— Upper plot: contour plot for the y - component of vector potential A (flux function) in the $x - z$ plane for an initial distribution of ambient arcade-like magnetic field. The field has a maximum $B_{max}(x_0 = 0, z_0 = 0) = 100$ G. Middle plot: initial symmetric profiles of the radial velocity V_z , and density n . The respective maxima (at $x=0$) are ~ 2 km/s and $10^{12} cm^{-3}$. Lower plot corresponds to time evolution of initial flow: $V_z(t, z = 0) = V_{0z} \sin(\pi t/t_0)$; $V_z(t > t_0) = 0$; $t_0 = 100$ s.

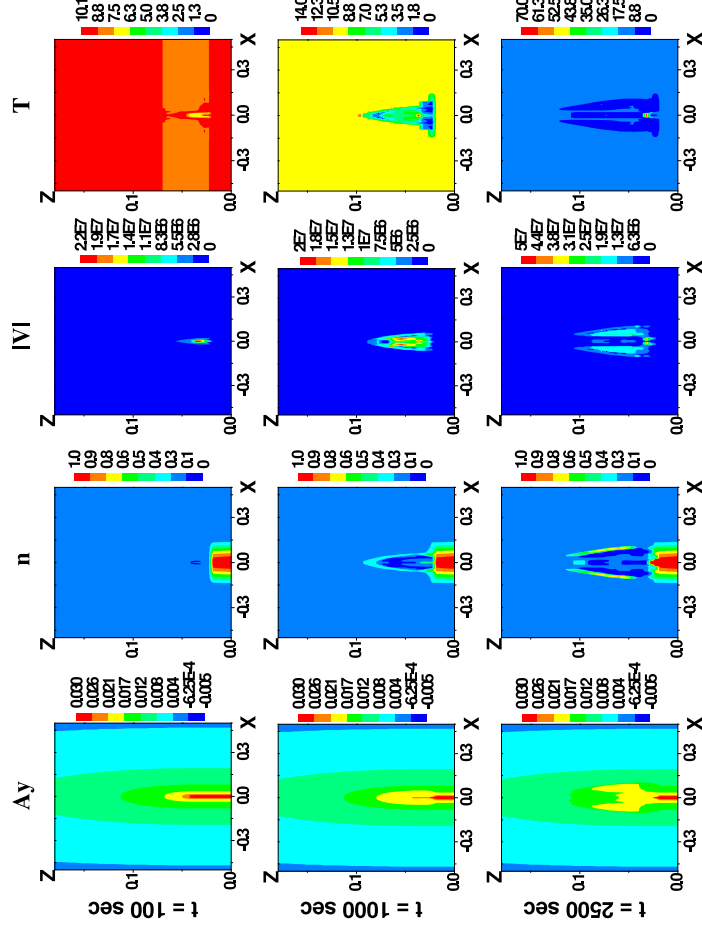


Fig. 2

Fig. 2.— $x - z$ contour plots at 3 time-frames: $t = 100$ s; 1000 s; 2500 s for the dynamical evolution of A_y (first panel from the left), n (second panel), $|\mathbf{V}|$ (third panel) and T (last panel) for flow – arcade field interaction. The realistic viscosity and heat-flux effects as well as the Hall term ($\alpha_0 = 3.3 \cdot 10^{-10}$) are included in the simulation. Primary flow (type displayed in Fig.1) is accelerated as it makes a way through the magnetic field with an arcade-like structure (Fig.1). The primary flow, locally sub-Alfvénic, is accelerated reaching significant speeds ($\gtrsim 100$ km/s) in a very short time ($\lesssim 100$ s). Initially the effect is strong in the strong field region (center of the arcade). There is a critical time ($\lesssim 1000$ s) when the accelerated flow bifurcates in 2; the original arcade field is deformed correspondingly. After the bifurcation, strong magnetic field localization areas, carrying currents, are created symmetrically about $x = 0$. Post-bifurcation daughter flows are localized in the newly created magnetic field localization areas. The maximum density of each daughter flow is of the order of the density of the mother-flow. Daughter-flows have distinguishable dimensions $\sim 0.05 R_s$. At $t \gtrsim 1000$ s, the velocities reach ~ 500 km/s or even greater ($\lesssim 800$ km/s) values. The distance from surface where it happens is $\gtrsim 0.01 R_s$. In the regions of daughter flows localization there is a significant cooling while the nearby regions are heated.

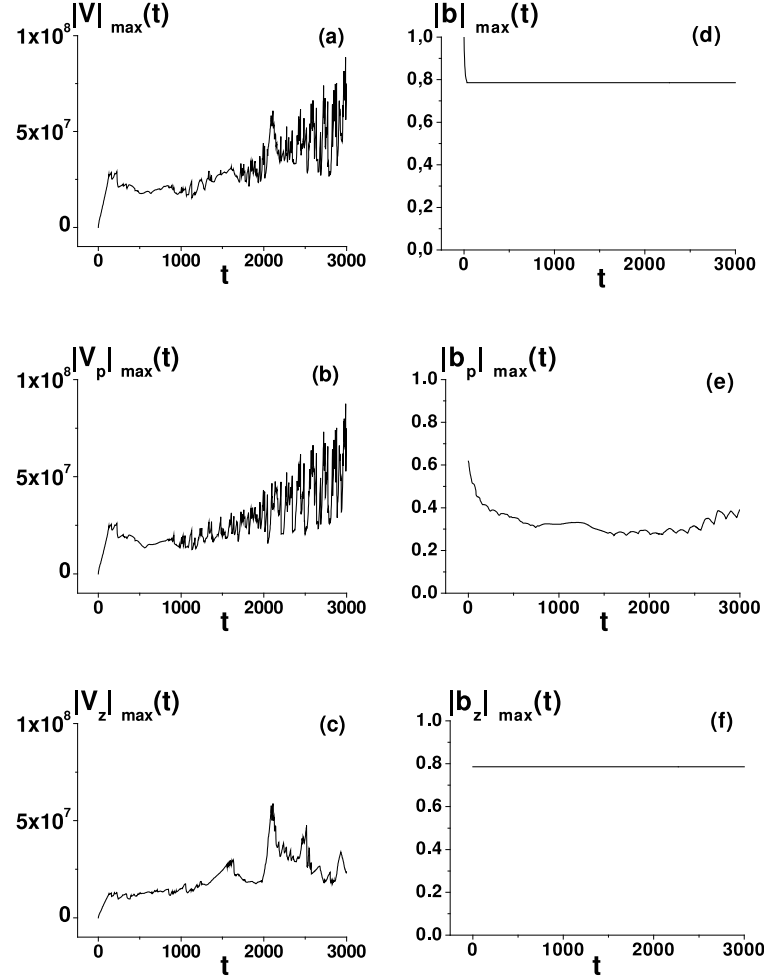


Fig. 3

Fig. 3.— Evolution of maximum values of $|\mathbf{V}|$, $|\mathbf{V}_p| = (V_x^2 + V_y^2)^{1/2}$, V_z ((a–c)) and $|\mathbf{b}|$, $|\mathbf{b}_p| = (b_x^2 + b_y^2)^{1/2}$, b_z ((d–f)) in time. (a),(d) – It is shown that much of the transfer from magnetic field energy happens while the first and very fast (~ 100 s) acceleration stage; (e),(b) – later, the dissipation of perpendicular (towards height) magnetic field fluctuations lead to the maintenance of the quasi-equilibrium fast perpendicular flows for a period of ~ 1000 s and then the effective acceleration of flow follows; (c),(f) – maximum value of magnetic field component along height is not changed and radial component of velocity field dissipates effectively. It should be emphasized that these maximum values of both field parameters change the localization dynamically and follow the relationship found analytically – fast flows (see Fig.2) are observed in the regions of large scale magnetic field maximum localization (initially given or later generated).